July 1, 2023

Detecting natural selection in trait-trait coevolution

Daohan Jiang[1,2*] and Jianzhi Zhang[1]

[1]Department of Ecology and Evolutionary Biology, University of Michigan, Ann Arbor, Michigan 48109, USA
[2]Present address: Department of Quantitative and Computational Biology, University of Southern California, Los Angeles, California 90007, USA

[*]Correspondence to
Daohan Jiang
Department of Quantitative and Computational Biology
University of Southern California
416F Ray R. Irani Hall
1050 Childs Way
Los Angeles, CA 9008, USA
Phone: 734-545-0764
Email: daohanji@usc.edu

Running title: Selection in trait-trait coevolution

Keywords: fly, morphology, mutation, modularity, pleiotropy, yeast

ABSTRACT

No phenotypic trait evolves independently of all other traits, but the cause of trait-trait coevolution is poorly understood. While the coevolution could arise simply from pleiotropic mutations that simultaneously affect the traits concerned, it could also result from multivariate natural selection favoring certain trait relationships. To gain a general mechanistic understanding of trait-trait coevolution, we examine the evolution of 220 cell morphology traits across 16 natural strains of the yeast *Saccharomyces cerevisiae* and the evolution of 24 wing morphology traits across 110 fly species of the family Drosophilidae, along with the variations of these traits among gene deletion or mutation accumulation lines (a.k.a. mutants). For numerous trait pairs, the phenotypic correlation among evolutionary lineages differs significantly from that among mutants. Specifically, we find hundreds of cases where the evolutionary correlation between traits is strengthened or reversed relative to the mutational correlation, which, according to our population genetic simulation, is likely caused by multivariate selection. Furthermore, we detect selection for enhanced modularity of the yeast traits analyzed. Together, these results demonstrate that trait-trait coevolution is shaped by natural selection and suggest that the pleiotropic structure of mutation is not optimal. Because the morphological traits analyzed here are chosen largely because of their measurability and thereby are not expected to be biased with regard to natural selection, our conclusion is likely general.

BACKGROUND

Many phenotypic traits covary during evolution. For example, the logarithm of brain weight and that of body weight show a nearly perfect linear relationship across mammals [1, 2]. In theory, four processes may explain such trait-trait coevolution. First, it could arise simply from pleiotropic mutations that simultaneously influence these traits with a more or less constant ratio of effects [3-5], as has been previously shown empirically [6-10]. Second, trait covariation could arise from the linkage disequilibrium between genes controlling these traits [5, 11-13], but such trait covariation is expected to be restricted to closely related individuals due to the deterioration of linkage disequilibrium as a result of recombination. If the linkage disequilibrium is stably maintained due to, for example, chromosomal inversion, the involved linked genes can be regarded as a supergene with mutational pleiotropy [13]. For this reason, linkage disequilibrium is negligible except for trait covariation among closely related individuals. Third, shared ancestry can also create apparent trait correlations across lineages, which, however, can be explained away when the phylogenetic relationships are taken into account in correlation analysis [14]. Finally, trait covariation could be a result of natural selection for particular trait relationships that are advantageous, a phenomenon known as correlational selection or multivariate selection [2, 15-20].

Despite a long-standing interest in trait correlation in evolution [2, 13, 21], which is also referred to as phenotypic integration in the literature [22, 23], our understanding of the roles of mutation and selection in trait-trait coevolution remains limited. Most studies on the subject focused on a small number of traits that are physiologically or ecologically important [24], such as skull anatomy characters [25-30], behavioral syndrome (i.e., sets of correlated behavioral traits) [31, 32], and ecological or organismal traits correlated with the metabolic rate [33-37]; hence, they may not provide a general, unbiased picture of trait-trait coevolution. Additionally, it is the trait correlation resulting from standing genetic variation and its effect on adaptation that have received the most attention [38-44]. But, because standing genetic variation could have been influenced by selection [40], the resulting trait correlation may not inform the correlation produced by mutation. Not knowing the mutational correlation hinders a full understanding of the contribution of selection.

Related to trait-trait correlation is the concept of modularity. It has been hypothesized that it is beneficial for organisms to have a modular organization such that functionally related

90 traits belonging to the same module covary and genotypes and/or phenotypes that lead to low
91 fitness are less likely to occur [21, 25, 45-47]. Although modularity is a well-recognized feature
92 of many trait correlation networks, the relative contribution of selection and mutational
93 pleiotropy to modularity has not been assessed at the phenome scale [46-48].
94 To gain a general mechanistic understanding of trait-trait coevolution, we study the
95 phenotypic correlations for a large number of trait pairs at the levels of mutation and long-term
96 evolution; natural selection is inferred when the evolutionary correlation between traits cannot be
97 fully explained by the mutational correlation. We also ask if the overall pattern of trait
98 correlation (i.e., phenotypic integration) differ at the two levels. Our primary data include 220
99 cell morphology traits of the budding yeast *Saccharomyces cerevisiae* that have been measured
100 in 4817 single-gene deletion lines [49], 89 mutation accumulation (MA) lines (for a subset of
101 187 traits) [50], and 16 natural strains with clear phylogenetic relationships [49, 51]. These traits
102 were quantified from fluorescent microscopic images of triple-stained cells and were originally
103 chosen for study because of their measurability regardless of potential roles in evolution and
104 adaptation [49]. Subsequent studies found that these cell morphological traits are correlated with
105 the yeast mitotic growth rate (i.e., a proxy for fitness) to varying degrees [7]. Hence, these traits
106 may be considered representatives of phenotypic traits that have different contributions to
107 fitness. Previous analyses of these traits among natural strains unveiled signals of positive
108 selection on individual traits [52], but their potential coevolution has not been studied. While
109 studying these trait pairs can offer a general picture of trait-trait coevolution, we recognize that
110 the selective agent would be hard to identify should selection be detected, because the biological
111 functions of these traits (other than correlations with the growth rate) are generally unknown
112 [52]. To verify the generality of the findings from the yeast traits, we analyze another dataset
113 that includes 12 landmark vein intersections on the fly wings that have been measured in 150
114 MA lines of *Drosophila melanogaster* [9] and 110 Drosophilid species [53]. At last, using
115 computer simulations, we demonstrate how certain regimes of selection could explain the
116 observed differences between mutational and evolutionary correlations.
117
118 **RESULTS**
119 **Evolutionary correlations differ from mutational correlations for many trait pairs**

120 To investigate if trait correlations in evolution can be fully accounted for by the
121 correlations generated by mutation, we examined all pairs of the 220 yeast cell morphology traits
122 previously measured. For each pair of traits, we computed the mutational correlation COR_M,
123 defined as Pearson's correlation coefficient across 4,817 gene deletion lines (upper triangle in
124 **Fig. 1A**, **Data S1**), and evolutionary correlation COR_E, defined as Pearson's correlation
125 coefficient across 16 natural strains (lower triangle in **Fig. 1A**, **Data S1**) with their phylogenetic
126 relationships (**Fig. S1**) taken into account (see Materials and Methods). Note that the original
127 data contained 37 natural strains [51], of which 21 belong to the "mosaic" group [54, 55]—their
128 phylogenetic relationships with other *S. cereviase* strains vary among genomic regions—so
129 cannot be included in our analysis that requires considering phylogenetic relationships.
130 We found that the frequency distribution of COR_E across all trait pairs differs
131 significantly from that of COR_M (**Fig. 1B**), suggesting the action of selection. For each pair of
132 traits, we transformed the COR_M and COR_E to Z-scores using Fisher's r-to-Z transformation and
133 conducted Z-test to determine whether the two correlations are significantly different. Of the
134 24,090 trait pairs examined, 6743 pairs (or 28.0%) have a COR_E that deviates significantly from
135 COR_M at the false discovery rate (FDR) of 5% (**Table 1**, **Data S1**), suggesting that natural
136 selection has shaped the coevolution of many trait pairs. To investigate whether the above result
137 is biased because of the use of each trait in many trait pairs, we randomly arranged the 220 traits
138 into 110 non-overlapping pairs and counted the number of pairs with COR_E significantly
139 different from COR_M. This was repeated 1,000 times to yield 1,000 estimates of the proportion
140 of trait pairs with significantly different COR_E and COR_M. The middle 95% of these estimates
141 ranged from 14.5% to 40.1%, with the median estimate being 28.2%, almost identical to the
142 result (28.0%) from all pairwise comparisons. Hence, there is no indication that using
143 overlapping trait pairs has biased the estimate of the fraction of trait pairs with significantly
144 different COR_E and COR_M.
145 To further test selection, we simulated neutral evolution along the yeast tree 1000 times
146 under a Brownian motion model with the observed mutational covariance matrix M used as the
147 mutational input, generating 1,000 simulated datasets. Before the simulation, we confirmed that
148 the sampling error of our estimated M is negligible, likely because of the large number of
149 mutants used in M estimation (**Table S1**; see Materials and Methods). From each simulated
150 dataset, we calculated the number of trait pairs with COR_E significantly different from COR_M.

151 Only in 0.7% of the simulated data did we find this number equal to or greater than that from the
152 actual data (**Table 1**), indicating that the observed evolutionary correlations between traits
153 cannot be explained by the neutral Brownian motion model. The distribution of mutational
154 effects can be asymmetric and skewed [56] while it is assumed normal in the Brownian motion
155 model. Nevertheless, simulations showed that mutational bias will not render COR_E deviate
156 from COR_M in the absence of selection and will not enlarge the variance of COR_E (**Table S2**; see
157 Materials and Methods).
158 We divided the 6743 cases of significantly different COR_E and COR_M into three
159 categories. In the first category, the trait correlation generated by mutation is strengthened by
160 natural selection during evolution. A total of 2,727 trait pairs are considered to belong to this
161 "strengthened" category (**Table 1**) because they satisfy the following criteria: COR_E and COR_M
162 have the same sign and $|COR_E| > |COR_M|$, or COR_E and COR_M have different signs but only
163 COR_E is significantly different from 0 (at the nominal *P*-value of 0.05) (**Fig. 2A**). In the second
164 category, the trait correlation generated by mutation is weakened by natural selection during
165 evolution. A total of 1,221 trait pairs satisfying the following criteria are classified into this
166 "weakened" category (**Table 1**): COR_E and COR_M have the same sign and $|COR_E| < |COR_M|$, or
167 COR_E and COR_M have different signs but only COR_M is significantly different from 0 (**Fig. 2B**).
168 In the last category, the trait correlation generated by mutation is reversed in sign by natural
169 selection during evolution. A total of 2,795 trait pairs satisfying the following criteria are in this
170 "reversed" category (**Table 1**): COR_E and COR_M have different signs and are both significantly
171 different from 0 (**Fig. 2C**).
172 To assess the robustness of the selection signals detected, we repeated the above analysis
173 using COR_M estimated from 89 mutation accumulation (MA) lines [43] (**Fig. S2A**, **Data S1**).
174 Again, the overall frequency distribution across all trait pairs differs significantly between COR_E
175 and COR_M (**Fig. S2B**). We found that 5,146 trait pairs exhibit a significantly different COR_E
176 from the corresponding COR_M (**Table 1**, **Data S1**), supporting a role of selection in the
177 coevolution of many trait pairs. When comparing the analysis using COR_M from gene deletion
178 lines and that using COR_M from MA lines, we found 990 trait pairs to exhibit selection signals
179 and fall into the same category in both analyses, including 275 pairs in the "strengthened"
180 category, 223 pairs in the "weakened" category, and 574 pairs in the "reversed" category. All of
181 these numbers substantially exceed the corresponding expected random overlaps ($P < 0.001$

182 based on 1,000 random draws in each case; the medians across the 1,000 draws are 271, 68 and
183 163, respectively), suggesting the reliability of both analyses. Although mutations in MA lines
184 are more natural than those in gene deletion lines, the number of MA lines is much smaller than
185 the number of gene deletion lines and only 187 of the original 220 traits were measured in the
186 MA lines. For these reasons, we focused on the COR_M estimated from the gene deletion lines in
187 subsequent analyses.

188 To examine the generality of the above yeast-based findings, we analyzed the 24 wing
189 morphology traits of Drosophilid flies. The COR_M and COR_E have been previously estimated
190 from 150 MA lines [9] and 110 Drosophilid species, respectively (**Fig. S3A**, **Data S1**). The
191 overall frequency distribution across all trait pairs differs significantly between COR_E and COR_M
192 (**Fig. S3B**). Of the 276 pairs of traits, 144 (52.2%) showed a significant difference between
193 COR_E and COR_M (**Table 1**, **Data S1**), indicating widespread actions of selection in the
194 coevolution of fly wing morphology traits.

195 Together, these results demonstrate that, for many trait pairs, mutational and evolutionary
196 correlations between morphological traits are more different than expected under neutrality.
197 This observation suggests an important role of selection in shaping the strength and/or direction
198 of trait correlation in evolution.

199

200 **Effects of different selection regimes on trait-trait coevolution**

201 The strengthened, weakened, and reversed trait correlations in evolution may have
202 resulted from different selection regimes. Below we consider various selection regimes that
203 could potentially explain these types of difference between COR_M and COR_E (**Fig. 3**). First,
204 when a specific allometric relationship between two traits is selectively favored, the population
205 mean trait values are expected to be concentrated near the fitness ridge or the optimal allometric
206 line, resulting in a strong evolutionary correlation between the traits (i.e., a high $|COR_E|$) (**Fig.
207 3A**). Unless COR_M is already similar to COR_E, we expect to see strengthened or reversed COR_E
208 depending on COR_M. Second, if there is a single fitness peak for an optimal combination of trait
209 values and if there is sufficiently strong stabilizing selection on the optimal phenotype, the
210 population mean phenotype should be restricted within a small range of the optimal phenotype in
211 all directions in the phenotypic space regardless of the mutational variance. Consequently,
212 COR_E is expected to be close to 0, which could account for a weakened evolutionary correlation

213 relative to the mutational correlation (**Fig. 3B**). Finally, if the fitness optimum varies across
214 lineages in a random fashion, the steady-state COR_E will be close to zero, potentially leading to
215 the weakening of the evolutionary correlation relative to the mutational correlation (**Fig. 3C**).
216 To verify these predictions, we simulated the evolution of two traits. Under each
217 parameter set, we simulated 50 independent replicate lineages and computed the correlation
218 coefficient, or COR_E, between the traits across the replicate lineages at the end of the simulated
219 evolution. This was repeated 200 times to obtain an empirical distribution of COR_E. To evaluate
220 the difference between COR_M and COR_E, we examined the location of COR_M in the distribution
221 of COR_E; a significant ($P < 0.05$) difference is inferred if COR_M is in the left or right 2.5% tail of
222 the COR_E distribution.
223 As expected, in the absence of selection, the distribution of COR_E is centered around
224 COR_M (first block in **Table 2**). When a specific allometric relationship is selectively favored, a
225 high $|COR_E|$ always emerges regardless of the COR_M used, resulting in either strengthened or
226 reversed evolutionary correlations ($P < 0.005$ for all parameter sets examined; the second to fifth
227 blocks in **Table 2**). By contrast, stabilizing selection of an optimal phenotype leads to weakened
228 correlation across replicate lineages when $|COR_M|$ is not small (sixth block in **Table 2**). Finally,
229 when different lineages have different phenotypic optima that are randomly picked from the
230 standard bivariate normal distribution, weakened evolutionary correlations are generally
231 observed except when COR_M is close to zero (bottom block in **Table 2**). These results suggest
232 that the strengthened and reversed evolutionary correlations of yeast and fly morphological traits
233 are likely caused by selections of allometric relationships, while the weakened correlations are
234 likely caused by selections of individual traits either when there is a single optimal phenotype or
235 when the optimal phenotype randomly varies among lineages.
236
237 **Selection for enhanced modularity of yeast morphological traits**
238 While all of the above analyses focused on individual trait pairs, here we ask whether the
239 overall trait correlation across divergent lineages is stronger or weaker than that created by
240 mutation. As a measure of the overall level of trait correlation (i.e., overall integration), we
241 calculated the variance of eigenvalues (V_{eigen}) of the correlation matrix from divergent lineages
242 and mutants, respectively. A greater V_{eigen} corresponds to a stronger overall correlation between
243 traits because the eigenvalues become less evenly distributed as the absolute values of the

correlation coefficients become larger [57]. However, the sample size (i.e., the number of strains) in the estimation of the correlation matrix also influences V_{eigen}; a matrix estimated from a smaller sample naturally tends to have fewer positive eigenvalues and greater V_{eigen}. To exclude the influence of this factor, we randomly sampled the mutant strains to obtain 5000 control datasets. Because the rank number of the evolutionary correlation matrix is 15 for the yeast data (i.e., 15 positive eigenvalues), each control dataset also consists of 15 randomly drawn strains such that the corresponding mutational correlation matrix also has 15 positive eigenvalues. We examined the location of the observed V_{eigen} in this distribution and computed a *P*-value based on this location (see Materials and Methods). For the yeast traits, V_{eigen} of the observed evolutionary correlation matrix exceeds that in 96% of control datasets ($P = 0.08$ in a two-tailed test; **Table 3**). Furthermore, only two of the 5000 control datasets have V_{eigen} significantly different from that of the observed evolutionary correlation matrix (Fligner-Kileen test). Hence, there is little evidence for a difference between the overall evolutionary correlation and the overall mutational correlation in yeast. For the fly data, the number of positive eigenvalues is unlimited by the sample size for both the evolutionary and mutational correlation matrices, hence we directly compared V_{eigen} between the two matrices, but found them to be similar ($P = 0.459$, Figner-Kileen test; **Table 3**). We also compared the overall integration between yeast and flies using $V_{eigen}/(n\text{-}1)$, where n is the number of traits examined. $V_{eigen}/(n\text{-}1)$ equals 0.157 and 0.268 for the yeast mutational and evolutionary matrices, respectively, whereas the corresponding values in flies are 0.153 and 0.190, respectively.

In addition to the overall level of trait correlation, we asked whether the correlational structure of traits exhibits different levels of modularity among divergent lineages when compared with that among mutants. To this end, we used a covariance ratio (*CR*) test [58] that compares covariance within and between pre-defined modules (see Materials and Methods). Specifically, we calculated *CR* for the evolutionary covariance matrix and compared it to the *CR* distribution based on 5000 mutational covariance matrices estimated from the randomly drawn subsets of mutants aforementioned. We treated the three non-overlapping categories of the yeast morphological traits—actin traits, nucleus traits, and cell wall traits [49]—as three modules (**Data S1**). We found that the *CR* of the evolutionary covariance matrix exceeded that of every control dataset ($P < 0.001$; **Table 3**), suggesting natural selection for increased modularity in evolution.

275

276 **DISCUSSION**

277 By comparing the trait-trait correlation across mutants (COR_M) with that across divergent
278 lineages (COR_E) for 24,090 pairs of yeast cell morphology traits and 276 pairs of fly wing
279 morphology traits, we detected the action of natural selection in trait-trait coevolution. The
280 fraction of trait pairs showing evidence for selection is substantially higher in the fly (52%) than
281 yeast (28%) data ($P < 10^{-4}$, chi-squared test). This is at least in part caused by a difference in
282 statistical power, because the number of strains/species used for estimating COR_E is much
283 greater for the fly (110) than yeast (16) data. It is likely that a higher fraction than 28% of the
284 yeast trait pairs are subject to selection in their coevolution. Furthermore, our comparison
285 between COR_E and COR_M intends to test selection on trait correlations common among the
286 evolutionary lineages considered. If different evolutionary lineages have different trait
287 correlations, the COR_E estimated from all lineages may not be significantly different from COR_M
288 even when selection occurs in some or all of the lineages. In other words, our test is expected to
289 underestimate the proportion of trait pairs subject to selection.

290 One potential biological explanation of the yeast-fly disparity in the prevalence of
291 correlational selection is divergence time: the fly species represent a group that is tens of
292 millions of years old while the yeast strains diverged from each other much more recently [53-
293 55]. It is known that genetic correlations predict evolutionary correlations better over shorter
294 timescales [38]. Similarly, selection might have had more time to decouple the pattern of
295 evolutionary divergence from the mutational input in the flies but not yet in the yeast strains.

296 While we assumed that the mutants used carry all designed or natural mutations,
297 extremely deleterious mutations such as lethal mutations are not represented. However, because
298 such mutations are quickly selectively purged in natural populations, they should only be present
299 transiently and are presumably unlikely to contribute to long-term evolution. Hence, their
300 absence from our mutant data should not qualitatively alter our results.

301 We demonstrated by simulations that various selection regimes can explain differences
302 between COR_M and COR_E. In particular, strengthened or reversed COR_E relative to COR_M can
303 occur when a specific allometric relationship is preferred, while weakened COR_E can occur
304 under directional or stabilizing selection of individual traits. A notable difference between the
305 simulation results and empirical observations is that the simulations tend to end up with extreme

306 values of $|COR_E|$ (i.e., close to either 1 or 0) except in the case of neutrality, whereas the
307 empirically observed $|COR_E|$ is usually less extreme even when COR_M and COR_E are
308 significantly different. This is due to the fact that the simulation results usually represent steady-
309 state correlations across lineages. That is, the mean phenotype of each lineage is at or near the
310 corresponding optimum (if any); consequently, $|COR_E|$ is close to 1 when the optimum is a line
311 and close to 0 when the optimum is a single combination of two trait values. However, the
312 population mean phenotypes may not be close to their optima in some strains because of recent
313 changes of the optima or the sparsity of mutations toward the optima, the latter of which is well
314 known as a potential hindrance to adaptation [38, 42, 43, 59]. Another possibility is the
315 existence of a wide range of preferred allometry such that there is no strong selection for extreme
316 $|COR_E|$. Finally, selection may not result in the preferred allometry between two traits because
317 of the constraints from unconsidered traits [60].
318 It is worth noting that the yeast natural strains had been cultured in synthetic media
319 before phenotyping [51] while the mutant strains were all grown in the rich medium YPD [49,
320 50]. Hence, it remains a possibility that the difference between COR_E and COR_M reported here
321 contains a component caused by the environmental difference in phenotyping. Notwithstanding,
322 our analysis suggests that this component is small (see Materials and Methods), which is
323 expected because both media are meant to provide an ideal, stress-free environment for yeast
324 growth. This said, future phenotyping in the same medium will be needed to validate our
325 findings.
326 While selection was detected for many trait pairs, a large fraction of trait pairs, especially
327 in the yeast data, do not show a significant difference between COR_E and COR_M. These trait
328 pairs may be divided into two groups. In the first group, COR_E and COR_M are actually different,
329 but the difference is not found significant due to the limited statistical power. As mentioned, we
330 believe that a substantial fraction of yeast trait pairs belong to this category due to the relatively
331 low statistical power in detecting the difference between COR_E and COR_M in the yeast data. In
332 the second group, COR_E truly equals COR_M, which could result from one of the following three
333 scenarios. First, the specific trait-trait correlation does not impact fitness so evolves neutrally.
334 Second, the two traits have an intrinsic, immutable relationship (such as the hypothetical traits of
335 body size and twice the body size), so will yield equal COR_E and COR_M; this possibility can be
336 tested by examining the correlation of the two traits across isogenic individuals that show non-

337 heritable phenotypic variations [61]. The last and perhaps the most interesting scenario is that
338 the trait-trait correlation impacts fitness and hence has driven the optimization of COR_M via a
339 second-order selection [52, 59, 62, 63] such that the first-order selection of mutations that affect
340 the two traits is no longer needed. However, the relative frequencies of these three scenarios are
341 unknown.

342 In addition to pairwise trait correlations, we tested hypotheses regarding the evolution of
343 overall phenotypic integration and modularity. In the yeast data, we observed a higher
344 modularity across natural strains than across mutants but did not find evidence for a change of
345 overall phenotypic integration in evolution. These results support the view of increasing
346 modularity during evolution [21, 25, 45, 46, 64] but also suggest that modularity is enhanced by
347 both strengthening trait-trait correlations within modules and weakening trait-trait correlations
348 across modules. We found the overall integration lower for the fly than yeast traits, but whether
349 this observation indicates a difference between different types of traits (i.e., cellular traits and
350 multicellular organisms' morphological traits) or between multicellular and unicellular
351 organisms requires analyzing more species and traits.

352 Our analysis compared COR_M estimated from one yeast strain (BY) with COR_E estimated
353 from 16 different strains, under the assumption of a constant COR_M across different strains.
354 While it is a common practice to assume that the mutational architecture is more or less constant
355 during evolution and to study phenotypic evolution by comparing mutational or genetic
356 (co)variances in one species with those among different species [53, 65, 66], genetic variations
357 affecting the genetic (co)variances of phenotypic traits have been reported [67-69]. As discussed
358 earlier, such genetic variations may allow second-order selection of COR_M. For instance, it has
359 been hypothesized that the optimization of mutational (co)variances driven by selection for
360 mutational robustness and/or adaptability can lead to modularity [21, 46]. It has indeed been
361 found in the study of *Drosophila* gene expression traits that variational modules identified from
362 mutants can be predicted to some extent by functional grouping of genes (i.e., Gene Ontology
363 terms), although there is still much difference between functional modules and modules resulting
364 from mutational pleiotropy, suggesting that optimization of the mutational architecture is far
365 from complete even if it did take place [47]. Even without second-order selection, COR_M could
366 still vary across strains because the pleiotropic effects of a mutation can vary by the environment
367 and genetic background [19, 70, 71]. Regardless, in the future, it would be desirable to measure

368 mutant phenotypes from multiple lineages to investigate whether COR_M evolves, how rapidly it
369 evolves, and whether its evolution is largely neutral or adaptive.
370 Our analysis of the yeast dataset is subject to a major limitation resulting from the
371 structure of the dataset. As many yeast strains are mosaic, only a small number of strains (16)
372 were used in our study. Most of the remaining strains fall in one clade (**Fig. S1**), which is the
373 Wine/European clade [54, 55]. That is, a substantial fraction of evolution along the yeast tree
374 took place on internal branch(es), which would further reduce the effective sample size [72]. As
375 a result, the COR_E estimate may not be very accurate, and the selection test suffers from low
376 statistical power. It would be desirable if more non-mosaic strains from non-Wine/European
377 clades are included. Another caveat regarding the calculation of COR_E is that correction
378 methods like independent contrast do not always sufficiently account for the tree structure and
379 can be susceptible to singular evolutionary events (e.g., shift of evolutionary rate in a clade) [73];
380 in our case, such a singular event could have taken place in the Wine/European clade after it had
381 split from other yeast strains.
382 In summary, we detected the action of natural selection in shaping trait-trait coevolution.
383 Because the traits analyzed here, especially the yeast traits, were chosen almost exclusively due
384 to their measurability, our results likely reflect a general picture of trait-trait coevolution.
385 Measuring these yeast traits in additional divergent natural strains with clear phylogenetic
386 positions could improve the statistical power and clarify whether the fraction of trait pairs whose
387 coevolution is shaped by selection is much greater than detected here. Finally, the detection of
388 selection for enhanced modularity of the yeast traits analyzed supports the hypothesis that
389 modularity is beneficial [21, 25]. The detection of selection in trait-trait coevolution and
390 selection for enhanced modularity suggests that the current pleiotropic structure of mutation is
391 not optimal. This nonoptimality could be due to the weakness of the second-order selection on
392 mutational structure and/or a high dependence of the optimal mutational structure on the
393 environment, which presumably changes frequently. Future studies on how the mutational
394 structure evolves will likely further enlighten the mechanism of trait-trait coevolution.
395
396 **CONCLUSION**
397 In this study, we analyzed morphological traits of yeast and flies and compared patterns
398 of trait-trait correlation at the levels of mutation and long-term evolution. In both datasets, we

399 discover that the evolutionary correlation differs significantly from the mutational correlation for
400 numerous trait pairs, revealing a role of natural selection in trait-trait coevolution. We also
401 provide evidence for selection for enhanced modularity of the yeast traits. Insights gained in this
402 study can be summarized as follows:

403 1) Can trait-trait correlations in long-term evolution be explained by mutations? Our
404 analyses showed that some correlations observed across divergent lineages differ
405 significantly from correlations created by mutations. In addition, the pattern of
406 phenotypic covariance among natural yeast strains has stronger modularity (i.e.,
407 stronger within-module correlations and/or weaker between-module correlations)
408 than among mutants. These observations together indicate that selection likely played
409 a role in shaping trait correlations in long-term evolution.
410 2) What evolutionary forces drive trait-trait correlation during evolution? Our
411 simulations show how various selection regimes render the pattern of correlation
412 during evolution different from that caused by mutation. Some types of differences,
413 including strengthening and reversal of correlations, are explained by selection for an
414 optimal allometric relationship, but not selection on individual traits.

415

416 **MATERIALS AND METHODS**

417 **Phenotypic data**

418 The *S. cerevisiae* cell morphology traits were previously measured by analyzing
419 fluorescent microscopic images. Three phenotypic datasets were compiled and analyzed in this
420 study, including (i) 220 traits measured in 4,718 gene deletion lines that each lack an
421 nonessential gene [49], (ii) the same 220 traits measured in 37 natural strains [51], and (iii) 187
422 of the 220 traits measured in 89 mutation accumulation (MA) lines [50]. When comparing
423 patterns of trait correlation between two datasets, we used traits available in both datasets. For
424 each deletion strain, many cells (95 on average) were phenotyped, and the average trait value of
425 all these cells were used to represent the strain in our analyses.

426 Three types of traits were measured in the deletion strains and the natural strains,
427 including actin traits (i.e., measurements based on dyed actin cytoskeleton), cell wall traits (i.e.,
428 measurements based on dyed mannoprotein and cell wall markers), and nucleus traits (i.e.,
429 measurements based on dyed nuclear DNA) [49, 51]. These three categories were treated as

430 three modules in our analysis of modularity. Only the cell membrane traits and nucleus traits
431 were measured in the MA lines [50].
432 Before the analyses, we first standardized all trait values by converting each trait value to
433 the natural log of the ratio of the original trait value to a reference such that the distributions
434 become approximately normal and suitable for the *Z*-test. The standardized value of the *i*th trait
435 in the *j*th strain is $\tilde{X}_{i,j} = ln\frac{X_{i,j}}{X_{i,r}}$, where $X_{i,j}$ is the original trait value and $X_{i,r}$ is the trait value of
436 the reference. For the gene deletion lines, the reference is the wild-type BY strain. For the MA
437 lines, the reference is the progenitor strain used in MA. For natural strains, the reference is the
438 same as the reference of the mutant strains to be compared with (i.e., wild-type BY or progenitor
439 of the MA lines).
440 The locations of 12 vein intersections on the fly wing were previously measured in 150
441 MA lines of *Drosophila melanogaster* and a mutational covariance matrix was estimated [9].
442 Because each intersection is described by two coordinates, which are counted as two traits, there
443 are 24 traits in this dataset. These traits were also measured in 110 Drosophilid species and an
444 evolutionary covariance matrix was estimated with species phylogeny taken into account [53].
445 Both matrices are based on log-scale trait values.
446
447 **Influence of the sampling error on the correlational structure**
448 To evaluate the influence of sampling error on the estimated mutational covariance
449 matrix (i.e., the *M* matrix) of yeast or fly, we took samples (vectors of phenotypes) from the
450 multivariate distribution of *M* (4,817 samples for yeast gene deletion data and 150 samples for
451 fly MA data), estimated a covariance matrix ($\widetilde{M}$) from these samples, and calculated Pearson's
452 correlation coefficient between the eigenvalues of *M* and $\widetilde{M}$. For instance, for the yeast data, *M*
453 and $\widetilde{M}$ each has 220 eigenvalues, and we calculated the correlation between these two sets of
454 eigenvalues as a measurement of similarity between *M* and $\widetilde{M}$. This was repeated 1,000 times
455 and the distribution of the correlation coefficient was used to evaluate the potential impact of
456 sampling error on *M*.
457
458 **Impact of the environmental difference on the correlational structure of the yeast traits**

459 Because the natural strains of yeast had been grown in synthetic media before
460 phenotyping [51] while the mutant strains were all grown in the rich medium YPD [49, 50], we
461 tested whether this environmental difference affected the correlational structure of the yeast
462 morphological traits under consideration. Specifically, we examined whether the phenotype of
463 the BY strain grown in synthetic media (referred to as "synthetic phenotype" for short) falls in
464 the distribution of 123 biological replicates of BY grown in YPD (referred to as "YPD
465 phenotypes" for short). The phenotypes were normalized in the way described earlier with the
466 mean phenotype of the YPD replicates used as the reference. We decomposed YPD phenotypes
467 into principal components (PCs) and focused on the first three PCs, which together explained
468 67.5% of the variance among the 123 YPD phenotypes. We then calculated the values of the
469 three PC traits of the synthetic phenotype. The synthetic phenotype is in the central 95% of the
470 distribution of the YPD phenotypes for each of the three PC traits, indicating a lack of major
471 effect of the difference between synthetic and YPD media on the correlational structure of the
472 yeast traits concerned.
473
474 **Comparison between mutational and evolutionary correlations**
475 To take into account the phylogenetic relationships among yeast strains in estimating
476 COR_E, we utilized a distance-based tree previously inferred [55] (**Fig. S1**). Strains with mosaic
477 origins inferred in the same study [55] were removed before analysis, resulting in 16 remaining
478 natural strains. Because the BY strain was not included in the data file in that study [55], W303,
479 a laboratory strain closely related to BY, was chosen to represent BY. We obtained the
480 evolutionary covariance matrix using the *ratematrix* function from the R package *geiger* [74,
481 75], which calculates evolutionary covariances using the independent contrast method [14]. The
482 evolutionary covariance matrix was then converted to the corresponding correlation matrix.
483 To test whether the observed pairwise trait correlation at the level of evolutionary
484 divergence is significantly different from that expected by mutation alone for each pair of traits,
485 we first converted both correlations to Z-scores by $Z = \frac{1}{2}[ln\ (1+r)\ -ln\ (1-r)]$, where r is
486 the correlation coefficient. The testing statistic was then computed by $Z = \frac{Z_E - Z_M}{\sqrt{\frac{1}{n_E-3}+\frac{1}{n_M-3}}}$, where Z_E
487 and Z_M are Z-scores converted from COR_E and COR_M, respectively, n_E is the number of
488 independent contrasts, which equals the number of natural strains minus one, and n_M is the

489 number of mutant strains. Two-sided *P*-value was calculated from each *Z* and converted to
490 adjusted *P*-value following the Benjamini-Hochberg procedure [76]. An adjusted *P*-value below
491 0.05 indicates selection.

492 To see how many trait pairs would show a significant difference between COR_E and
493 COR_M under neutrality, we simulated neutral evolution along the phylogenetic tree that had been
494 used in estimating COR_E. A Brownian motion model was used to simulate neutral phenotypic
495 evolution such that the amount of evolution in branch *i* is $M_i l$, where M_i is a vector sampled
496 from the multivariate normal distribution of the mutational covariance matrix *M* and l is the
497 branch length. Sampling was performed using the *rmvnorm* function in the R package *mvtnorm*
498 [77]. The starting value of each trait is 0 in all simulations. The phenotypic value of each strain
499 was obtained by adding up the amount of evolution on all branches ancestral to the strain. This
500 was repeated 1,000 times to generate 1,000 datasets.

501 To account for the difference in V_{eigen} caused by different sample sizes in estimating the
502 correlation matrices, we randomly sampled subsets of the gene deletion strains. Because the
503 evolutionary correlation matrix has a rank number of 15 and has 15 positive eigenvalues, each
504 subset consists of 15 strains randomly drawn from the 4718 gene deletion strains such that the
505 mutational correlation matrix computed from each subset of mutants also has 15 positive
506 eigenvalues. From each subset of strains, we computed V_{eigen}, leading to a null distribution of
507 V_{eigen}. The observed V_{eigen} from the evolutionary correlation matrix is then compared with the
508 null distribution; a significant difference is inferred if the observed value falls in either the left or
509 right 2.5% tail.

510 To test whether there exists a significant modular structure among traits, we performed
511 the covariance ratio (*CR*) test. For each pair of predefined modules, traits were first re-ordered
512 such that traits belonging to each module were located in the upper-left and lower-right corners
513 of the covariance matrix, respectively, and $CR = \sqrt{\frac{trace(M_{12}M_{21})}{\sqrt{trace(M_{11}^{*}M_{11}^{*})+trace(M_{22}^{*}M_{22}^{*})}}}$, where M_{12} and
514 M_{21} are the upper-right and lower-left sections of the original covariance matrix, respectively,
515 containing all between-module covariances, M_{11}^{*} is the upper-left section with diagonal elements
516 replaced by zeros, M_{22}^{*} is the lower-right section with diagonal elements replaced by zeros, and
517 $trace(M)$ denotes the trace, or the sum of diagonal elements, of matrix *M* [58]. Because three
518 modules were defined in the yeast data, the average of all pairwise *CR* values was used to

represent the overall modularity. A test for selection on *CR* was performed following the test of selection on V_{eigen}.

Computer simulation of trait-trait coevolution under selection

In each simulation, we considered a pair of traits with equal amounts of mutational variance V_{M}, which is set to be 0.01. The mutational covariance matrix is thus $M = \begin{bmatrix} V_M & COV_M \\ COV_M & V_M \end{bmatrix} \begin{bmatrix} V_M & V_M COR_M \\ V_M COR_M & V_M \end{bmatrix}$, where COV_{M} is the mutational covariance. The number of mutations is a random Poisson variable with the mean equal to 1. The phenotypic effect of a mutation is drawn from the multivariate normal distribution of *M* using the *rmvnorm* function in the R package *mvtnorm* [77]. The starting phenotype is (0, 0) in all simulations.

We considered a Gaussian fitness function of $f = exp\ (-\frac{D^2}{2})$, where *f* is the fitness and *D* is the distance between the current phenotype and the optimal phenotype. When there is a single fitness peak (i.e., the fitness optimum is a single point), *D* is the Euclidean distance defined by $\sqrt{{d_1}^2 + {d_2}^2}$, where d_1 and d_2 are the distances between the current phenotypic values of the two traits and their corresponding optima, respectively. When there is a fitness ridge (i.e., the fitness optimum is a line), *D* is the shortest distance from the current phenotype to the fitness ridge. The selection coefficient *s* equals $\frac{f}{f_{WT}} - 1$, where *f* and f_{WT} are the fitness values of the mutant and wild type, respectively. The fixation probability of a newly arisen mutant is $P_f = \frac{1-exp\ (-2s)}{1-exp\ (-2N_e s)}$ in a haploid population [78], where the effective population size N_{e} was set at 10^4. After each unit time, the phenotypic effect of each mutation is added to the population mean with a probability of $N_e P_f$; this probability is treated as 1 when $N_e P_f > 1$ or when there is no selection as in the latter case $P_f = \frac{1}{N_e}$. Combinations of parameters used in the simulations are listed in Table 2.

In simulations where different lineages were assigned different optima, each lineage's optimum was obtained by independently drawing the optimal values of the two traits from the standard normal distribution. Before conducting simulations, we confirmed that the optima of the two traits are not correlated (correlation coefficient = 0.0882, *P* = 0.54, *t*-test).

547 **Computer simulation of trait-trait coevolution under mutational bias**

548 To investigate the effect of mutational bias on trait correlation, we introduced the bias
549 coefficient B. Each mutation, after being sampled from a multivariate normal distribution
550 described above, was rescaled using B. Let the mutational effect be $m = (m_1, m_2)$, where m_1 and
551 m_2 are the effects on trait 1 and trait 2, respectively. The rescaled mutational effect, $\widetilde{m}$, is
552 obtained by

553 $$\widetilde{m} = \begin{cases} mB & (m_1 > 0) \\ \dfrac{m}{B} & (m_1 < 0) \end{cases}$$

554 Because mutational effects are first drawn from a pre-set multivariate normal distribution
555 and then rescaled, we examined if COR_{M} estimated from the rescaled effects ($\widetilde{COR_M}$) is different
556 from the pre-set value of COR_{M}. For each pre-set value of COR_{M}, we obtained
557 $\widetilde{COR_M}$ from 5,000 rescaled mutations. This was repeated 200 times with different random
558 mutations, yielding 200 $\widetilde{COR_M}$ estimates. A series of different B values were used in the
559 simulation (**Table S2**). For comparison, we also estimated B from yeast gene deletion lines and
560 found the maximal B of any trait to be 1.503. To estimate B for a trait from the yeast gene
561 deletion lines, we respectively calculated the mean trait value of all deletion lines with positive
562 trait values and mean trait value of all deletion lines with negative values. We then computed the
563 ratio of their absolute values with the greater absolute value used as the numerator. The square
564 root of the ratio is B. We found that COR_{M} is always near the center of the distribution of these
565 200 $\widetilde{COR_M}$ estimates (**Table S2**). Hence, mutational bias will not bias our test.

566 All analyses in this study were conducted in R [79].

567

568 **LIST OF ABBREVIATIONS**

569 MA: mutation accumulation.

570 CR: covariance ratio.

571

572 **DECLARATION**

573 **Ethics approval and consent to participate**

574 Not applicable.

575

576 **Consent for publication**

Not applicable.

Availability of data and materials

The datasets generated and/or analysed during the current study are available at https://github.com/RexJiangEvoBio/Trait-Correlation.

Competing interest

The authors declare that they have no competing interests.

Funding

This work was supported by U.S. National Institutes of Health grant R35GM139484 to J.Z. D.J. was supported by Predoctoral Fellowship of Rackham Graduate School, University of Michigan while working on the project.

Authors' contributions

D.J. and J.Z. designed the study. D.J. performed the analyses and prepared all figures. D.J. and J.Z. wrote the paper.

Acknowledgements

We thank members of the Zhang lab and Dr. Matthew Pennell for valuable comments.

REFERENCES

1. Gould SJ: **Allometry and Size in Ontogeny and Phylogeny**. *Biol Rev* 1966, **41**(4):587-640.
2. Lande R: **Quantitative Genetic Analysis of Multivariate Evolution, Applied to Brain - Body Size Allometry**. *Evolution* 1979, **33**(1):402-416.
3. Lande R: **The Genetic Covariance between Characters Maintained by Pleiotropic Mutations**. *Genetics* 1980, **94**(1):203-215.
4. Wagner GP: **Multivariate Mutation-Selection Balance with Constrained Pleiotropic Effects**. *Genetics* 1989, **122**(1):223-234.
5. Wagner GP, Zhang J: **The pleiotropic structure of the genotype-phenotype map: the evolvability of complex organisms**. *Nature Reviews Genetics* 2011, **12**(3):204-213.

6. Dugand RJ, Aguirre JD, Hine E, Blows MW, McGuigan K: **The contribution of mutation and selection to multivariate quantitative genetic variance in an outbred population of Drosophila serrata**. *Proc Natl Acad Sci U S A* 2021, **118**(31).
7. Ho WC, Zhang J: **The genotype-phenotype map of yeast complex traits: basic parameters and the role of natural selection**. *Mol Biol Evol* 2014, **31**(6):1568-1580.
8. McGuigan K, Collet JM, McGraw EA, Ye YH, Allen SL, Chenoweth SF, Blows MW: **The nature and extent of mutational pleiotropy in gene expression of male Drosophila serrata**. *Genetics* 2014, **196**(3):911-921.
9. Houle D, Fierst J: **Properties of Spontaneous Mutational Variance and Covariance for Wing Size and Shape in Drosophila Melanogaster**. *Evolution* 2013, **67**(4):1116-1130.
10. McGuigan K, Collet JM, Allen SL, Chenoweth SF, Blows MW: **Pleiotropic mutations are subject to strong stabilizing selection**. *Genetics* 2014, **197**(3):1051-1062.
11. Lande R: **The maintenance of genetic variability by mutation in a polygenic character with linked loci (Reprinted)**. *Genetics Research* 2007, **89**(5-6):373-387.
12. Gardner KM, Latta RG: **Shared quantitative trait loci underlying the genetic correlation between continuous traits**. *Mol Ecol* 2007, **16**(20):4195-4209.
13. Saltz JB, Hessel FC, Kelly MW: **Trait Correlations in the Genomics Era**. *Trends Ecol Evol* 2017, **32**(4):279-290.
14. Felsenstein J: **Phylogenies and the Comparative Method**. *Am Nat* 1985, **125**(1):1-15.
15. Roff DA, Mostowy S, Fairbairn DJ: **The evolution of trade-offs: Testing predictions on response to selection and environmental variation**. *Evolution* 2002, **56**(1):84-95.
16. Sinervo B, Svensson E: **Correlational selection and the evolution of genomic architecture**. *Heredity (Edinb)* 2002, **89**(5):329-338.
17. Shoval O, Sheftel H, Shinar G, Hart Y, Ramote O, Mayo A, Dekel E, Kavanagh K, Alon U: **Evolutionary trade-offs, Pareto optimality, and the geometry of phenotype space**. *Science* 2012, **336**(6085):1157-1160.
18. Bolstad GH, Cassara JA, Marquez E, Hansen TF, van der Linde K, Houle D, Pelabon C: **Complex constraints on allometry revealed by artificial selection on the wing of Drosophila melanogaster**. *P Natl Acad Sci USA* 2015, **112**(43):13284-13289.
19. Svensson EI, Arnold SJ, Burger R, Csillery K, Draghi J, Henshaw JM, Jones AG, De Lisle S, Marques DA, McGuigan K *et al*: **Correlational selection in the age of genomics**. *Nat Ecol Evol* 2021.
20. Svensson EI: **Multivariate selection and the making and breaking of mutational pleiotropy**. *Evol Ecol* 2022, **36**:807-828.
21. Wagner GP, Altenberg L: **Perspective: Complex Adaptations and the Evolution of Evolvability**. *Evolution* 1996, **50**(3):967-976.
22. Olson EC, Miller RL: **Morphological integration**, Pbk. edn. Chicago: University of Chicago Press; 1999.
23. Pigliucci M: **Phenotypic integration: studying the ecology and evolution of complex phenotypes**. *Ecol Lett* 2003, **6**(3):265-272.
24. Kingsolver JG, Hoekstra HE, Hoekstra JM, Berrigan D, Vignieri SN, Hill CE, Hoang A, Gibert P, Beerli P: **The strength of phenotypic selection in natural populations**. *Am Nat* 2001, **157**(3):245-261.

654 25. Goswami A, Smaers JB, Soligo C, Polly PD: **The macroevolutionary consequences of**
655 **phenotypic integration: from development to deep time**. *Philos Trans R Soc Lond B*
656 *Biol Sci* 2014, **369**(1649):20130254.
657 26. Porto A, Sebastiao H, Pavan SE, VandeBerg JL, Marroig G, Cheverud JM: **Rate of**
658 **evolutionary change in cranial morphology of the marsupial genus Monodelphis is**
659 **constrained by the availability of additive genetic variation**. *J Evol Biol* 2015,
660 **28**(4):973-985.
661 27. Simon MN, Machado FA, Marroig G: **High evolutionary constraints limited adaptive**
662 **responses to past climate changes in toad skulls**. *Proc Biol Sci* 2016, **283**(1841).
663 28. Watanabe A, Fabre AC, Felice RN, Maisano JA, Muller J, Herrel A, Goswami A:
664 **Ecomorphological diversification in squamates from conserved pattern of cranial**
665 **integration**. *Proc Natl Acad Sci U S A* 2019, **116**(29):14688-14697.
666 29. Fabre AC, Bardua C, Bon M, Clavel J, Felice RN, Streicher JW, Bonnel J, Stanley EL,
667 Blackburn DC, Goswami A: **Metamorphosis shapes cranial diversity and rate of**
668 **evolution in salamanders**. *Nat Ecol Evol* 2020, **4**(8):1129-1140.
669 30. Navalon G, Marugan-Lobon J, Bright JA, Cooney CR, Rayfield EJ: **The consequences**
670 **of craniofacial integration for the adaptive radiations of Darwin's finches and**
671 **Hawaiian honeycreepers**. *Nature Ecology & Evolution* 2020, **4**(2):270-+.
672 31. Sih A, Bell A, Johnson JC: **Behavioral syndromes: an ecological and evolutionary**
673 **overview**. *Trends Ecol Evol* 2004, **19**(7):372-378.
674 32. Dochtermann NA, Dingemanse NJ: **Behavioral syndromes as evolutionary**
675 **constraints**. *Behav Ecol* 2013, **24**(4):806-811.
676 33. Martin RD: **Relative brain size and basal metabolic rate in terrestrial vertebrates**.
677 *Nature* 1981, **293**(5827):57-60.
678 34. Brown JH, Gillooly JF, Allen AP, Savage VM, West GB: **Toward a metabolic theory of**
679 **ecology**. *Ecology* 2004, **85**(7):1771-1789.
680 35. Glazier DS: **A unifying explanation for diverse metabolic scaling in animals and**
681 **plants**. *Biol Rev* 2010, **85**(1):111-138.
682 36. Pettersen AK, White CR, Marshall DJ: **Metabolic rate covaries with fitness and the**
683 **pace of the life history in the field**. *P Roy Soc B-Biol Sci* 2016, **283**(1831).
684 37. White CR, Marshall DJ, Alton LA, Arnold PA, Beaman JE, Bywater CL, Condon C,
685 Crispin TS, Janetzki A, Pirtle E *et al*: **The origin and maintenance of metabolic**
686 **allometry in animals**. *Nat Ecol Evol* 2019, **3**(4):598-603.
687 38. Schluter D: **Adaptive radiation along genetic lines of least resistance**. *Evolution* 1996,
688 **50**(5):1766-1774.
689 39. Steppan SJ, Phillips PC, Houle D: **Comparative quantitative genetics: evolution of the**
690 **G matrix**. *Trends Ecol Evol* 2002, **17**(7):320-327.
691 40. Arnold SJ, Burger R, Hohenlohe PA, Ajie BC, Jones AG: **Understanding the Evolution**
692 **and Stability of the G-Matrix**. *Evolution* 2008, **62**(10):2451-2461.
693 41. Walsh B, Blows MW: **Abundant Genetic Variation plus Strong Selection =**
694 **Multivariate Genetic Constraints: A Geometric View of Adaptation**. *Annu Rev Ecol*
695 *Evol S* 2009, **40**:41-59.
696 42. Agrawal AF, Stinchcombe JR: **How much do genetic covariances alter the rate of**
697 **adaptation?** *P Roy Soc B-Biol Sci* 2009, **276**(1659):1183-1191.
698 43. Blows MW, Mcguigan K: **The distribution of genetic variance across phenotypic**
699 **space and the response to selection**. *Mol Ecol* 2015, **24**(9):2056-2072.

44. Walter GM, Aguirre JD, Blows MW, Ortiz-Barrientos D: **Evolution of Genetic Variance during Adaptive Radiation**. *Am Nat* 2018, **191**(4):E108-E128.
45. Wagner GP: **A research programme for testing the biological homology concept**. *Novartis Found Symp* 1999, **222**:125-134; discussion 134-140.
46. Wagner GP, Pavlicev M, Cheverud JM: **The road to modularity**. *Nature Reviews Genetics* 2007, **8**(12):921-931.
47. Collet JM, McGuigan K, Allen SL, Chenoweth SF, Blows MW: **Mutational Pleiotropy and the Strength of Stabilizing Selection Within and Between Functional Modules of Gene Expression**. *Genetics* 2018, **208**(4):1601-1616.
48. Wang Z, Liao BY, Zhang JZ: **Genomic patterns of pleiotropy and the evolution of complexity**. *P Natl Acad Sci USA* 2010, **107**(42):18034-18039.
49. Ohya Y, Sese J, Yukawa M, Sano F, Nakatani Y, Saito TL, Saka A, Fukuda T, Ishihara S, Oka S *et al*: **High-dimensional and large-scale phenotyping of yeast mutants**. *P Natl Acad Sci USA* 2005, **102**(52):19015-19020.
50. Geiler-Samerotte KA, Zhu YO, Goulet BE, Hall DW, Siegal ML: **Selection Transforms the Landscape of Genetic Variation Interacting with Hsp90**. *Plos Biol* 2016, **14**(10).
51. Yvert G, Ohnuki S, Nogami S, Imanaga Y, Fehrmann S, Schacherer J, Ohya Y: **Single-cell phenomics reveals intra-species variation of phenotypic noise in yeast**. *BMC Syst Biol* 2013, **7**:54.
52. Ho WC, Ohya Y, Zhang JZ: **Testing the neutral hypothesis of phenotypic evolution**. *P Natl Acad Sci USA* 2017, **114**(46):12219-12224.
53. Houle D, Bolstad GH, van der Linde K, Hansen TF: **Mutation predicts 40 million years of fly wing evolution**. *Nature* 2017, **548**(7668):447-+.
54. Liti G, Carter DM, Moses AM, Warringer J, Parts L, James SA, Davey RP, Roberts IN, Burt A, Koufopanou V *et al*: **Population genomics of domestic and wild yeasts**. *Nature* 2009, **458**(7236):337-341.
55. Peter J, De Chiara M, Friedrich A, Yue JX, Pflieger D, Bergstrom A, Sigwalt A, Barre B, Freel K, Llored A *et al*: **Genome evolution across 1,011 Saccharomyces cerevisiae isolates**. *Nature* 2018, **556**(7701):339-344.
56. Hodgins-Davis A, Duveau F, Walker EA, Wittkopp PJ: **Empirical measures of mutational effects define neutral models of regulatory evolution in Saccharomyces cerevisiae**. *Proc Natl Acad Sci U S A* 2019, **116**(42):21085-21093.
57. Pavlicev M, Cheverud JM, Wagner GP: **Measuring Morphological Integration Using Eigenvalue Variance**. *Evol Biol* 2009, **36**(1):157-170.
58. Adams DC: **Evaluating modularity in morphometric data: challenges with the RV coefficient and a new test measure**. *Methods Ecol Evol* 2016, **7**(5):565-572.
59. Hansen TF, Houle D: **Measuring and comparing evolvability and constraint in multivariate characters**. *J Evolution Biol* 2008, **21**(5):1201-1219.
60. Houle D, Jones LT, Fortune R, Sztepanacz JL: **Why does allometry evolve so slowly?** *Integr Comp Biol* 2019, **59**(5):1429-1440.
61. Geiler-Samerotte KA, Li S, Lazaris C, Taylor A, Ziv N, Ramjeawan C, Paaby AB, Siegal ML: **Extent and context dependence of pleiotropy revealed by high-throughput single-cell phenotyping**. *Plos Biol* 2020, **18**(8).
62. Wagner A: **Robustness and evolvability in living systems**. Princeton, NJ: Princeton University Press; 2005.

63. Jones AG, Arnold SJ, Burger R: **Evolution and stability of the G-matrix on a landscape with a moving optimum**. *Evolution* 2004, **58**(8):1639-1654.
64. Clune J, Mouret JB, Lipson H: **The evolutionary origins of modularity**. *Proc Biol Sci* 2013, **280**(1755):20122863.
65. Ackermann RR, Cheverud JM: **Detecting genetic drift versus selection in human evolution**. *Proc Natl Acad Sci U S A* 2004, **101**(52):17946-17951.
66. Lynch M: **The Rate of Morphological Evolution in Mammals from the Standpoint of the Neutral Expectation**. *Am Nat* 1990, **136**(6):727-741.
67. Jerison ER, Kryazhimskiy S, Mitchell JK, Bloom JS, Kruglyak L, Desai MM: **Genetic variation in adaptability and pleiotropy in budding yeast**. *Elife* 2017, **6**.
68. Jones AG, Burger R, Arnold SJ: **Epistasis and natural selection shape the mutational architecture of complex traits**. *Nat Commun* 2014, **5**:3709.
69. Pavlicev M, Kenney-Hunt JP, Norgard EA, Roseman CC, Wolf JB, Cheverud JM: **Genetic variation in pleiotropy: Differential epistasis as a source of variation in the allometric relationship between long bone lengths and body weight**. *Evolution* 2008, **62**(1):199-213.
70. Pavlicev M, Cheverud JM: **Constraints Evolve: Context Dependency of Gene Effects Allows Evolution of Pleiotropy**. *Annual Review of Ecology, Evolution, and Systematics, Vol 46* 2015, **46**:413-434.
71. Wei X, Zhang J: **Environment-dependent pleiotropic effects of mutations on the maximum growth rate r and carrying capacity K of population growth**. *Plos Biol* 2019, **17**(1):e3000121.
72. Ané C: **Analysis of comparative data with hierarchical autocorrelation**. *Annals of Applied Statistics* 2008, **2**(3):1078-1102.
73. Uyeda JC, Zenil-Ferguson R, Pennell MW: **Rethinking phylogenetic comparative methods**. *Syst Biol* 2018, **67**(6):1091-1109.
74. Pennell MW, Eastman JM, Slater GJ, Brown JW, Uyeda JC, FitzJohn RG, Alfaro ME, Harmon LJ: **geiger v2.0: an expanded suite of methods for fitting macroevolutionary models to phylogenetic trees**. *Bioinformatics* 2014, **30**(15):2216-2218.
75. Revell LJ, Harmon LJ, Langerhans RB, Kolbe JJ: **A phylogenetic approach to determining the importance of constraint on phenotypic evolution in the neotropical lizard Anolis cristatellus**. *Evol Ecol Res* 2007, **9**(2):261-282.
76. Benjamini Y, Hochberg Y: **Controlling the False Discovery Rate - a Practical and Powerful Approach to Multiple Testing**. *J R Stat Soc B* 1995, **57**(1):289-300.
77. Genz AB, F.; Miwa, T.; Mi, X.; Leisch, F.; Scheipl, F.; Hothorn, T.: **mvtnorm: Multivariate Normal and t Distributions. R package version 1.1-0, https://CRAN.R-project.org/package=mvtnorm.** 2020.
78. Kimura M: **On the probability of fixation of mutant genes in a population**. *Genetics* 1962, **47**:713-719.
79. R Core Development Team: **R: A language and environment for statistical computing**. 2010.

790 Table 1. Numbers of trait pairs with significantly different COR_E and COR_M in the yeast and fly data.

	Yeast						Fly (276 trait pairs)		
	COR_M from gene deletion lines (24,090 trait pairs)			COR_M from MA lines (17,391 trait pairs)					
	Observed[a]	Expected[b]	Fraction[c]	Observed	Expected	Fraction	Observed	Expected	Fraction
Strengthened	2727	145	3%	2395	17	3.5%	68	0	0%
Weakened	1221	78	1.4%	1348	6	0.1%	48	0	0%
Reversed	2795	51	0%	1403	2	0%	28	0	0%
Total	6743	302.5	0.7%	5146	31	0.7%	144	0	0%

791 [a]Number of trait pairs with significantly different COR_M and COR_E inferred by a Z-test.
792 [b]Number of trait pairs that show a significant difference between COR_M and COR_E derived from neutral Brownian
793 motion simulations. The median from 1000 simulations is shown.
794 [c]Fraction of the 1000 Brownian motion simulations where the number of trait pairs with significantly different
795 COR_M and COR_E exceeds the number under the "observed" column.
796
797

Table 2. Parameters and results of simulations of trait-trait coevolution.

Optimum	COR_M	Median COR_E at the end of simulation	Fraction of simulations with $COR_E > COR_M$	COR_E compared with COR_M
No optimum	0.9	0.900	49.5%	No difference
	0.5	0.495	47.5%	No difference
	0.1	0.113	55.5%	No difference
$y = x$ *	0.9	1.000	100%	Strengthened
	0.5	1.000	100%	Strengthened
	0.1	1.000	100%	Strengthened
$y = 0.5x$	0.9	1.000	100%	Strengthened
	0.5	1.000	100%	Strengthened
	0.1	1.000	100%	Strengthened
$y = -0.5x$	0.9	-0.995	0%	Reversed
	0.5	-0.999	0%	Reversed
	0.1	-1.000	0%	Reversed
$y = -x$	0.9	-0.997	0%	Reversed
	0.5	-0.999	0%	Reversed
	0.1	-1.000	0%	Reversed
(0, 0)	0.9	0.0213	0%	Weakened
	0.5	0.00142	0.5%	Weakened
	0.1	-0.0109	24%	No difference
Drawn from $\boldsymbol{N(0,1)}$	0.9	0.0895	0%	Weakened
	0.5	0.0874	0%	Weakened
	0.1	0.0866	6%	No difference

*x and y respectively represent the values of the two traits considered.

Table 3. Overall phenotypic integration (V_{eigen}) and modularity (CR) at the levels of mutation and evolutionary divergence. Values at the level of mutation for yeast are medians of 1,000 control datasets. P-values for yeast are computed from locations of the observed values in the corresponding distributions of 5000 control datasets, while the P-value for fly is from a Fligner-Killeen test.

Statistic	Taxon	Mutation	Divergence	P-value
V_{eigen}	Yeast	34.414	58.656	0.0788
	Fly	3.530	4.359	0.459
CR	Yeast	0.649	0.997	< 0.001

811 **Figure legends**

812 **Figure 1.** Mutational (COR_M) and evolutionary (COR_E) correlations for all pairs of the 220 yeast
813 morphological traits. COR_M is based on yeast gene deletion lines. (A) COR_M (upper triangle)
814 and COR_E (lower triangle) for all pairs of traits ordered according to their IDs. (B) Frequency
815 distributions of COR_M and COR_E across all trait pairs. The two distributions are significantly
816 different ($P < 10^{-10}$, Kolmogorov–Smirnov test).

817

818 **Figure 2.** Examples of yeast trait pairs with COR_E significantly different from the corresponding
819 COR_M. (A) An example of evolutionarily strengthened correlation. (B) An example of
820 evolutionarily weakened correlation. (C) An example of evolutionarily reversed correlation.
821 Each blue dot represents a gene deletion line (a.k.a. mutant) while each red dot represents an
822 independent contrast derived from natural strains. Blue and red lines are linear regressions
823 between the standardized values of the two traits in mutants and independent contrasts,
824 respectively, while the dotted blackline shows the diagonal ($y = x$). Trait IDs are shown along
825 the axes. All COR_M and COR_E values shown are significantly different from 0 except when
826 indicated by "NS" in the parentheses.

827

828 **Figure 3.** Schematic illustration of predictions made by models of trait-trait coevolution. Each
829 circle represents the equilibrium mean phenotype of two hypothetical traits (trait 1 and trait 2) of
830 a diverging lineage. (A) When a specific allometric relationship is selectively favored, the
831 population mean phenotypes are distributed along the fitness ridge (i.e., the optimal allometric
832 line shown in red), resulting in a strong trait correlation across lineages. (B) When a specific
833 value is selectively favored for each trait, the population mean phenotypes are concentrated near
834 the optimal phenotype (marked by the red cross) and the trait correlation across lineages is weak.
835 (C) When different lineages have different optimal phenotypes (marked by red crosses) that are
836 randomly distributed, the trait correlation across lineages is weak.

837
838

839 **Figure 1**
840
841 A

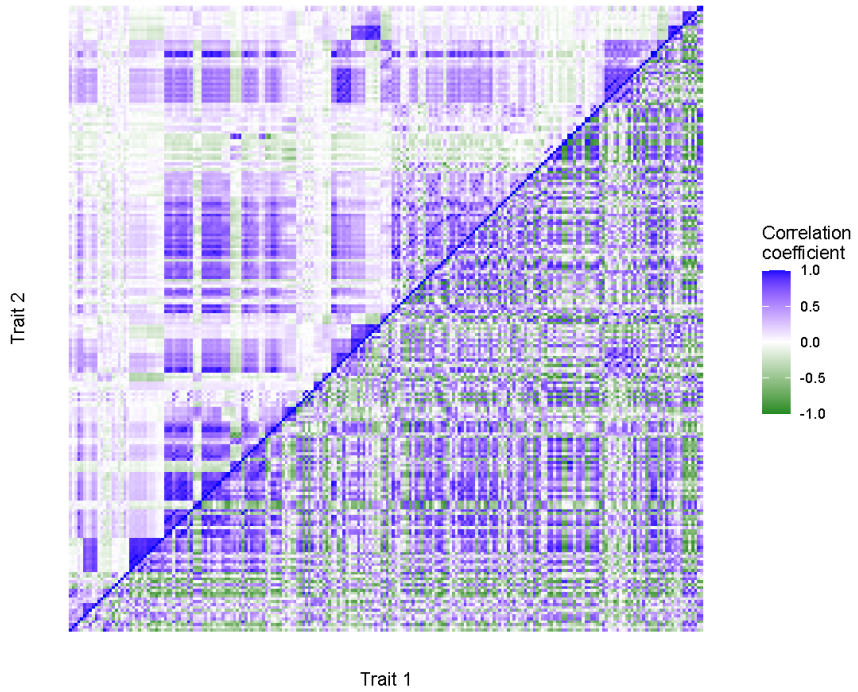

842
843 B

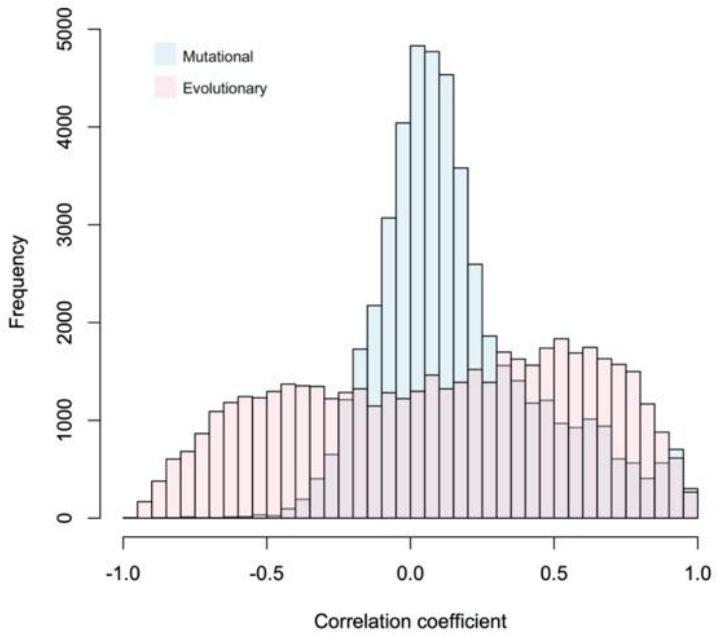

844
845
846
847

848 **Figure 2**

849

850 A

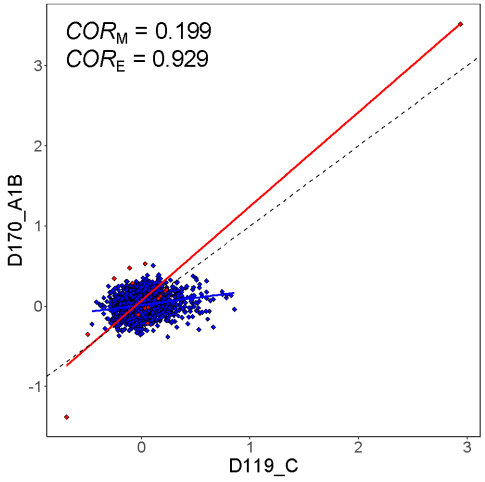

851

852 B

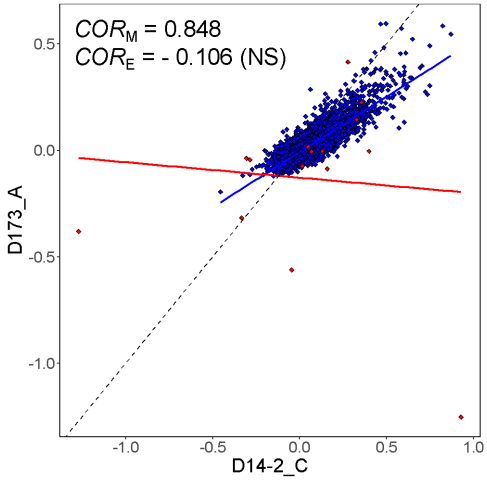

853

854 C

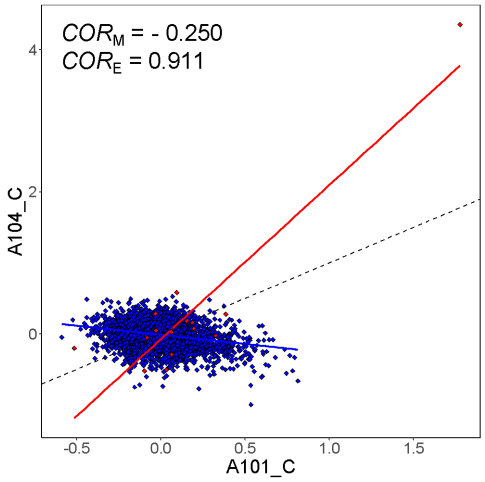

855

Figure 3

A

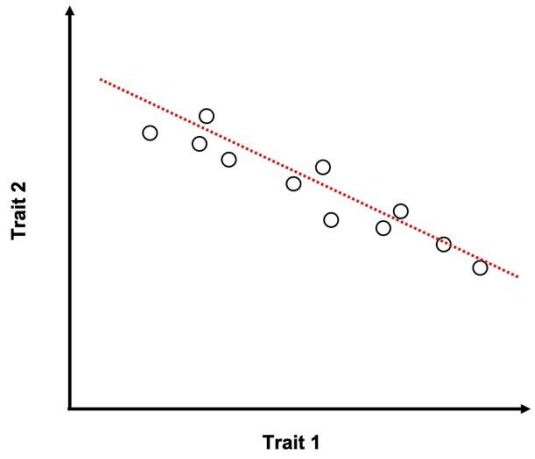

B

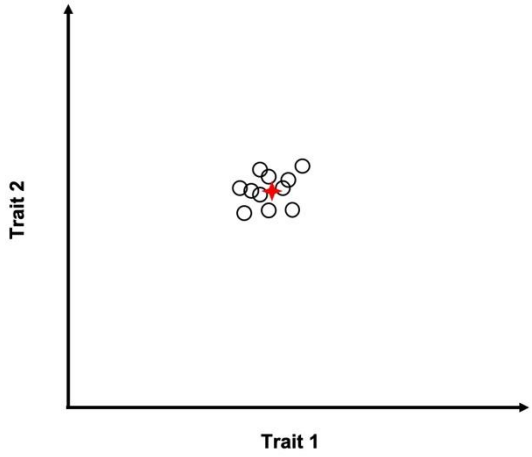
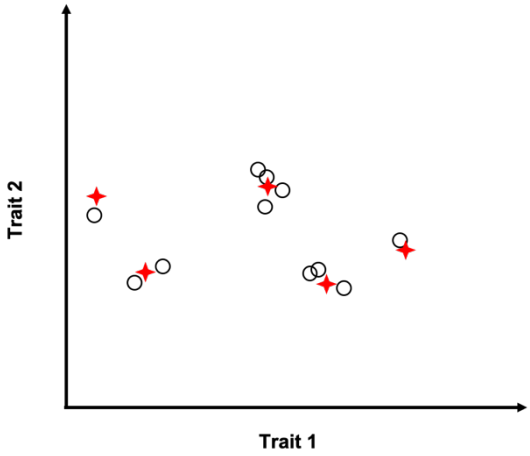
C